Dissolved organic matter dynamics in the pristine Krka River estuary (Croatia)

Saša Marcinek, Chiara Santinelli, Ana-Marija Cindrić, Valtere Evangelista, Margherita Gonnelli, N. Layglon, Stéphane Mounier, Véronique Lenoble, Dario Omanović

Dissolved organic matter dynamics in the pristine Krka River Estuary (Croatia)

Saša Marcinek[1,*], Chiara Santinelli[2], Ana-Marija Cindrić[1], Valtere Evangelista[2], Margherita Gonnelli[2], Nicolas Layglon[3], Stephane Mounier[3], Veronique Lenoble[3] and Dario Omanović[1]

[1] Ruđer Bošković Institute, Center for Marine and Environmental Research, Zagreb, Croatia
[2] CNR - Biophysics Institute, Pisa, Italy
[3] Mediterranean Institute of Oceanology, ECEM, Toulon University, La Garde, France
*Corresponding author: smarcin@irb.hr

Abstract

In many estuarine systems, riverine discharge is the main source of dissolved organic matter (DOM). In contrast, karstic Krka River, with self-purifying ability, is characterized by very low DOM concentrations (~30 µM) and a diluting effect on DOM in the estuary. Interestingly, within the estuary a marked in-situ production is observed, particularly in summer. Pristine nature of the estuary makes it a natural laboratory to study the DOM dynamics, originated from 3 sources: the river the seawater and in-situ production. With this work we aim at reporting the first information on DOM dynamics in the Krka estuary in two contrasting seasons, winter and summer 2019. The quality of DOM was assessed using absorbance and fluorescence measurements coupled with PARAFAC analysis. During winter, the estuary is characterized by extremely low DOC concentrations, for which optical properties indicate that is mainly of terrestrial origin. In summer, due to the low riverine discharge and high temperature, DOC concentrations are higher than in winter and a marked increase in absorption and protein-like fluorescence is observed in the estuary. The permanent stratification determines DOC accumulation in the surface layer with values up to 147 µM, suggesting a decoupling between production and removal processes. Our work opens intriguing questions about the main processes responsible for DOC accumulation in this system and highlights the need of new studies combing chemical and biological information.

Keywords: Chromophoric dissolved organic matter (CDOM), Dissolved organic carbon (DOC), Excitation-emission matrices (EEMs), PARAFAC, Krka River Estuary, in-situ production, Stratified estuary, Terrestrial DOM

1. Introduction

Dissolved organic matter (DOM) is one of the major components of aquatic ecosystems. Besides being source of energy and nutrients that supports life, it controls the functioning of biogeochemical cycles and ecological processes in the water column. Chromophoric/Colored Dissolved Organic Matter (CDOM) is the fraction of DOM capable of absorbing light at the UV and visible wavelengths. A fraction of CDOM, called fluorescent DOM (FDOM), can emit part of the absorbed light as fluorescence. Although they represent a small and not well defined fraction of the entire DOM pool, CDOM and FDOM are of vital interest for aquatic ecosystem functioning, since they are the main factor determining the light availability (penetration depth) in natural waters (Stedmon and Nelson, 2015). DOM composition is chemically very complex and cannot be easily characterized (Repeta, 2015). CDOM and FDOM studies, therefore, can be helpful in order to gain qualitative information on DOM pool, such as average aromaticity degree and molecular weight as well as the occurrence of humic-like, fulvic-like and protein-like substances. In the literature, FDOM has been also used to distinguish DOM sources and biological lability (Dainard et al., 2015; Fellman et al., 2011; Galletti et al., 2019; Lee et al., 2018; Osburn et al., 2012; Yamashita et al., 2011).

DOM in the oceans contain the largest pool of dissolved organic carbon (DOC) compared to all other ecosystems (Hansell et al., 2009). It, therefore, plays a crucial role in the global carbon cycle. DOM in the oceans is mainly produced in-situ, even if external sources (rivers, atmosphere and sediments) are crucial for the input of terrigenous (vascular plant detritus or soil humus) and anthropogenic (black carbon polycyclic aromatic hydrocarbon) DOM. River input is considered the main source of DOM to the coastal systems and inverse relationship between DOC and salinity is usually observed in these areas (Massicotte et al., 2017). The estuaries play a key role in riverine DOM input to the oceans, since they are the transition zones, where photochemical and/or biological processes can transform the riverine DOM before its input to the coastal ocean. In estuaries, DOM can be partially removed and replaced by the DOM produced by autochthonous processes, such as phytoplankton release or cell lysis (Gonnelli et al., 2013). Estuaries with low influence of seawater are largely controlled by changes in river flow and during periods of reduced discharge, autochthonous processes could gain importance in this environments (Dixon et al., 2014; Fellman et al., 2011; Santos et al., 2016). As an example, (Dixon et al., 2014) found that in Neuse River estuary lower input of allochthonous DOM and increased residence time of water allowed for the accumulation of autochthonous DOM. They also show that shallow microtidal estuaries can generate significant amount of autochthonous DOM which can possibly dominate the allocthonous input during low river flow.

Karst environments with self-purifying ability, such as the Krka River estuary, could deviate from common relationship of DOC and salinity by showing lower DOC values in the river than in the coastal seawater (Cindric et al., 2015). In these environments, during the periods of low river discharge, autochthonous processes could be more important than in estuaries with high riverine influence. Under the conditions of small terrestrial and negligible anthropogenic input (Cindric et al., 2015; Legovic et al., 1994), photochemical and biological processes are expected to strongly affect DOM pool, while the permanent stratification could further influence DOM distribution and dynamics (Santinelli et al., 2013). While the Krka River estuary is in general well characterized on its hydrology, biological status and trace metals behavior (Cetinic et al., 2006; Cindric et al., 2015; Knežević et al., 2019; Legovic, 1991; Pađan et al., 2019a; Pađan et al., 2019b; Supraha et al., 2014; Svensen et al., 2007; Zutic and Legovic, 1987), the organic matter dynamics has been only sporadically studied and to the best of our knowledge, no information about CDOM and FDOM dynamics is reported. In this study, we investigated DOM dynamics in the Krka River estuary during two contrasting periods of the year; February 2019, characterized by low production and high riverine input and July 2019, characterized by high solar irradiation, high production, and very low riverine discharge (Fig. S1) (Cetinic et al., 2006; Legovic et al., 1994). In coastal environments, characterized by high terrestrial and anthropogenic influence, high allochthonous input of DOM hinders the assessment of its dynamics. In the pristine Krka River estuary with low riverine influence, particularly during the summer, we had the opportunity to study DOM dynamics and optical properties of 3 different pools of DOM (terrestrial, marine and produced in-situ by biological activity).

2. Materials and methods

2.1. Study area

The Krka River estuary is situated in the Croatian coast of the Adriatic Sea. The Krka canyon is covered in limestone prone to karstation, as most of the Croatian coast. This process forms tufa barriers, which create lakes and waterfalls along the river flow. Estuary begins after the last and the biggest waterfall Skradinski Buk (46 m high). Map of the estuary, with its total length of 23.5 km, is presented in Fig. 1. Right plot shows bottom depth which ranges from 2 m below the Skradinski buk waterfalls (station 0) to 43 m at the mouth of the estuary. Prokljan Lake (station 5) and the Šibenik area (station 10) are two wider parts that stand out from generally narrow estuary. As a result of its specific geography and low tidal influence (~30 cm at the head and ~40 at the mouth of the estuary (Legovic et al., 1994)) estuary is permanently stratified. Surface Fresh/brackish Water Layer (FWL) is separated from the Sea Water Layer (SWL) by sharp halocline formed at a depth between 1.5 and 5 m. Extension of

the surface layer depends on the Krka River discharge, that has an average annual value of 52.9 m^3 s^{-1} (Buzancic et al., 2016). Seawater renewal results from its entrainment into the freshwater-seawater interface that pushes it toward the sea. In the widest parts of the estuary, during high river flow, seawater renewal time ranges between 50 and 100 days, whereas, during low river flow, seawater renewal time is up to 250 days (Legovic, 1991). Due to the tufa barriers, preceding the estuary, freshwater entering the estuary is exceptionally clean with low concentrations of nutrients, trace elements and terrigenous material (Cindric et al., 2015; Legovic et al., 1994). With an annual nutrient input of 55×10^6 mol N, 1.8×10^6 mol P and 36.4×10^6 mol Si, the estuary is a P-limited system (Grzetic et al., 1991; Svensen et al., 2007). According to (Cetinic et al., 2006) phytoplankton community is a rather typical coastal marine than estuarine community.

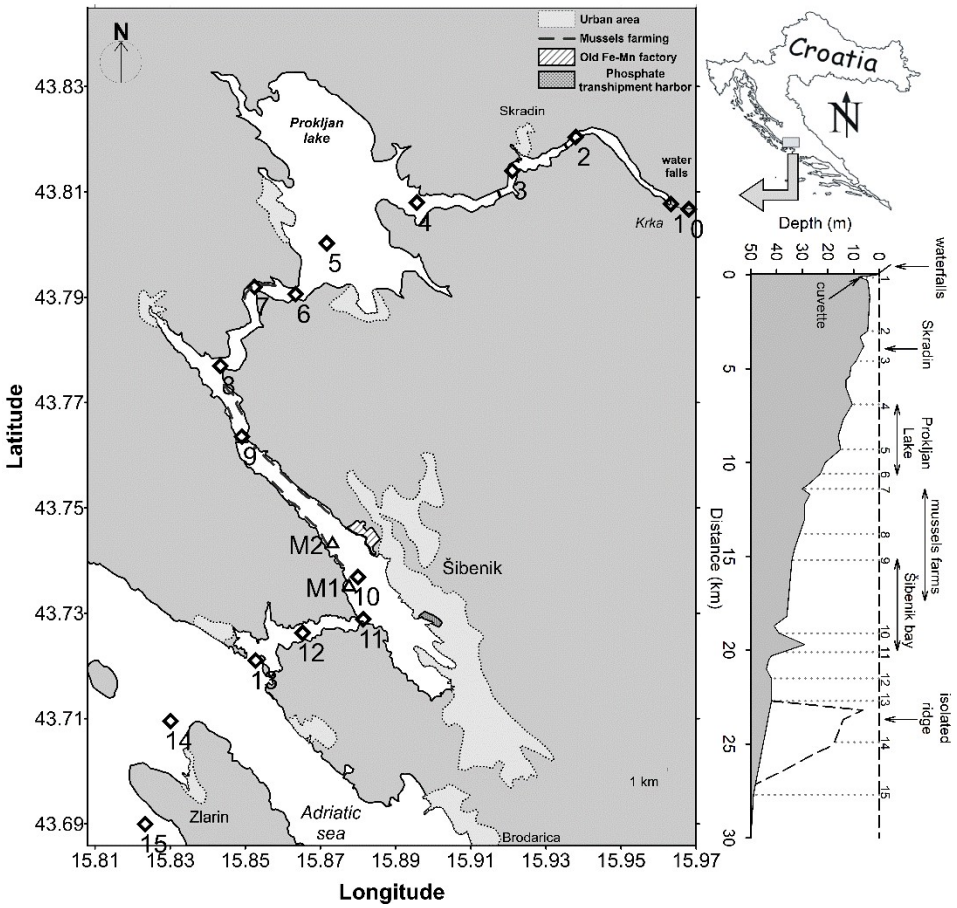

Figure 1. Map of the Krka River Estuary with marked sampling stations. Right plot shows horizontal bottom depth with marked sites and specific regions (Cindric et al., 2015).

2.2. Sampling stations and samples collection

Samples were collected at 16 stations along the estuary from Skradinski Buk waterfalls to the coastal area, south of the Island Zlarin (Fig. 1). Samples were collected in the surface

and bottom layer in winter (February 12th, 2019), during high Krka River flow, and summer (July 24th, 2019), during low Krka River flow (Fig. S1). Samples were collected, also, at 6 depths, chosen from the vertical salinity profiles (2 in FWL, 2 at freshwater-seawater interface and 2 in SWL) at station M1 (located in front of Martinska marine station) in February 2019 and at stations 5, M1 and M2 (located in the mussel farm) in July 2019 (Fig. 1). Additional 6 samples (K1-K6) were also collected in the Krka River, on July 22nd, 2019. The sampling was carried out when a phytoplankton bloom occurred in the Visovac Lake (station K4), preceding the Skradinski Buk waterfalls.

Vertical profiles of environmental parameters (salinity, temperature, oxygen saturation, turbidity, chlorophyll *a* (chl-*a*), Blue Green Algae (BGA) and pH) were measured by using the EXO2 multiparameter CTD probe (YSI). Apparent oxygen utilization (AOU) was calculated as difference between oxygen saturation and oxygen expected at given depth, temperature and salinity. Samples were collected using van Dorn type horizontal sampler (alfa or beta, Wildco) and immediately filtered on-board through a 0.22 µm CA filters (Sartorius) by using pre-cleaned syringe (5% v/v HNO_3, rinsed 3 times with Mili-Q water). Samples were stored at 4 °C in pre-cleaned (1% v/v HCl, rinsed 3 times with Mili-Q water) polycarbonate (Nalgene) bottles until the analysis, carried out within one month. Syringes, filters and bottles were rinsed with the sample before its collection. The filtration system (syringe + filter) was selected after repeated tests, since they did not contaminate samples for DOC, CDOM nor FDOM.

2.3. Dissolved organic carbon measurements

DOC concentration was determined by high temperature catalytic oxidation using a Shimadzu TOC-VCSN carbon analyzer. Prior to oxidation, samples were acidified with 2 M high purity HCl and purged for 3 min with pure air to remove inorganic carbon. In order to achieve satisfying analytical precision (±1%) up to 5 replicate injections were performed. At the beginning and the end of each analytical day, the system blank was measured using Milli-Q water and the functioning of the instrument was checked by comparison of data with DOC Consensus Reference Material (CRM) (Hansell, 2005) (batch #18/08-18, measured concentration: 43.7 ± 0.8 µM, n = 14 and batch #19/03-19, measured concentration: 40.5 ± 0.6 µM, n = 8). External calibration curve was measured with potassium hydrogen phthalate as the organic standard. For more details please refer to (Santinelli et al., 2015).

2.4. Absorbance measurements

UV-Vis spectra were measured using a JASCO Spectrophotometer V-550 with 10-cm Suprasil quartz cuvettes. Scan was performed between 230 and 800 nm using 1000 nm/min scan rate and 0.5 nm resolution. The spectrum of Milli-Q water, measured in the same conditions, was

used as blank and subtracted from each sample. UV-Vis spectra were treated using newly purpose-developed software package, ASFit (Omanović et al., 2019). In order to minimize light scattering interferences, baseline subtraction of average absorption between 650 and 700 nm was performed. Absorbance at 254 nm (A_{254}) was used as representative of CDOM pool and expressed as absorption coefficient (a_{254}) in Naperian units (Eq. 1)

$$a_{254} = 2{,}303 \cdot \frac{A_{254}}{l} \qquad (1)$$

where l is the path length expressed in meters. The specific UV absorbance at 254 nm ($SUVA_{254}$) was calculated by dividing the decadic absorbance coefficient at 254 nm by DOC concentration (mg C L^{-1}) and used as indicator of percentage of CDOM in the total DOM pool (Stedmon and Nelson, 2015). Spectral slope over 275–295 nm spectral range ($S_{275\text{-}295}$) was calculated using exponential model (Eq. 2) and used as proxy for average molecular weight (MW), aromaticity and humification degree (Helms et al., 2008) as well as a proxy of terrigenous DOC (Fichot and Benner, 2012).

$$a_{\lambda} = a_{\lambda_0} \cdot e^{-S(\lambda - \lambda_0)} \qquad (2)$$

where a_{λ} is the absorption coefficient at specific wavelength and λ_0 is the reference wavelength.

In order to study spectral differences among DOM pool, wavelength distribution of a spectral slopes expressed as spectral slope curve (*SSC*) (Loiselle et al., 2009) was used. Average SSCs of freshwater (n = 9) and seawater samples (n = 6) as well as SSC for few typical samples was obtained by calculating the spectral slopes for 20 nm intervals across 200-500 nm wavelength range. ASFit procedure is described in detail in (Omanović et al., 2019).

2.5. Fluorescence measurements

Fluorescence excitation-emission matrices (EEMs) were recorded using the Aqualog spectrofluorometer (Horiba- Jobin Ivon) in 10×10 mm^2 quartz cuvettes. EEMs were scanned at the excitation wavelengths range of 250-450 nm with 5 nm increments and emission wavelengths range of 212-619 nm with 3 nm increments. Excitation and emission slit-widths were both set at 5 nm. The blanks were checked every 5 samples by measuring EEM of Milli-Q water. As the fluorescence intensities measured in Milli-Q were negligible across the scanned range if compared to the fluorescence intensity measured in samples, the blank EEMs were not subtracted from samples. Fluorescence intensity values were normalized to Raman units (R.U.) using daily measured Raman peak of Mili-Q water (λ_{ex} = 350 nm, λ_{em} = 371–428 nm). Parallel factorial analysis (PARAFAC) was applied to identify the different

fluorescent components in the FDOM pool by using the decomposition routines for EEMs (drEEM) toolbox (version 0.2.0; (Murphy et al., 2013) for MATLAB (R2016a). PARAFAC was applied to the complete dataset (Dataset 1, 102 EEMs). EEMs were also separated according with the season: Dataset 2 (February 2019) and Dataset 3 (July 2019) and according with both season and layers, defined by salinity, (February 2019: S <20 - Dataset 4, S >37 - Dataset 5, July 2019: S <27 - Dataset 6, S >37 - Dataset 7) (Table 1.). Validated fluorescent components were identified as humic-like and protein-like substances by comparison with (i) commercial humic substances (Suwanne River fulvic acid and Pahokee Peat humic acid from International Humic Substances Society) and tryptophan from Sigma-Aldrich; (ii) similar components reported in the literature and (iii) matching spectra obtained from the OpenFluor database (Murphy et al., 2014) (Table S1).

3. Results

3.1. Environmental parameters

Salinity vertical distribution clearly shows two layers in both seasons: FWL (S<20) flows seaward, above the SWL (S>37) (Fig. 2A and C). In winter, water with low salinity (S<8) is clearly visible in the upper 5 m until station 12, very close to the sea. In contrast, in summer, due to very low discharge of the river, freshwater occupies only the upper 1.5 m and intense mixing with marine water starts upstream in the estuary (station 4). Stations 5 to 12 are characterized by intermediate salinity (S = 15-27).

Temperature vertical distribution is inverse in the 2 seasons (Fig. 2B and D). In February, Riverine Water (RW) and most of the FWL are characterized by average temperature of ~10 °C, whereas Sea Water (SW) and SWL have average temperature of 13 °C (Table 2). The maximum (15 °C) is recorded in the shallowest part of the estuary (stations 2-4) below 5 m. In July, RW has average temperature of 19 °C, and FWL is characterized by the highest temperature (26 °C), with values decreasing in seawater to reach a temperature of 17 °C below 14 m at stations 6-11.

In February, oxygen saturation closely resembles the distribution of salinity and temperature, with over saturation (>100%) at the freshwater-seawater interface, a minimum (70-75%) at stations 2-4 below 5 m and average values of 90% in SW (Fig. 3A). In July, oxygen oversaturation (120-160%) is observed in the river (stations K3-K6), and in the subsurface layer (1-5 m) at stations 2-9 and in Šibenik bay (station 10) at about 3 m (Fig. 3C). Hypoxia (<38%) occurs in the bottom layer of station 1, supporting the long residence time of this water (Cindric et al., 2015; Legovic, 1991).

As expected, chl-*a* is higher in July (4-5 µg/L) than in February (<3.5 µg/L) (Fig. 3B and D), when its maximum is observed at the halocline in Šibenik Bay (station 10). Surprisingly, in July high chl-*a* values are recorded not at the halocline but close to the bottom with a maximum (7 µg/L) in the middle of the estuary (station 8) between 20 and 23 m. In Visovac lake (station K4), where a phytoplankton bloom was observed prior to our sampling campaign, chl-*a* and dissolved oxygen show high values.

3.2. DOC and CDOM

DOC ranges between 35 and 76 µM in February and 30 and 148 µM (Fig. 4A and C). The lowest values are measured in RW in both seasons (35 µM in February at station 0 and 30 µM in July at station K1). Seawater is characterized by average concentrations of 63 µM in February and 60 µM in July (Table 2), in agreement with concentrations reported for open waters of the Mediterranean Sea (Catala et al., 2018; Galletti et al., 2019; Santinelli, 2015;

Santinelli et al., 2010). In July, the riverine water after the Skradinski Buk waterfalls (station 0) has higher DOC values (55 µM) than in January. A noteworthy result is the marked DOC increase in correspondence with the mixing between freshwater and seawater (stations 2-13), with a maximum (> 100 µM) at stations 5-7.

In both seasons, a_{254} shows higher average values in RW (2.6 m^{-1} in February and 2.2 m^{-1} in July) than in SW (1.6 m^{-1} in February and 1.7 m^{-1} in July) (Table 2 and Fig. 4B and D). Interestingly, a marked increase in absorption is observed in the middle part of the estuary where freshwater and seawater mix (stations 5-7). Here, a_{254} shows average values of 3.2 m^{-1} in winter and up to 4.2 m^{-1} in summer, clearly indicating net production of CDOM. In July, the maximum of a_{254} (6.4 m^{-1}) is at station 1 in the bottom sample, where hypoxia is observed (Fig. 3C).

In both seasons, $S_{275\text{-}295}$ is lower in RW (average values of 16.8 μm^{-1} in February and 16.6 μm^{-1} in July) than in SW (average values of 30.5 μm^{-1} in February and 29.3 μm^{-1} in July) (Table 2 and Fig. 5A and C). It is noteworthy that in July, in the bottom layer at station 1, where high a_{254} is observed, $S_{275\text{-}295}$ is low (17.4 μm^{-1}), suggesting the occurrence of material with high molecular weight and aromaticity degree (Helms et al., 2008).

As expected, $SUVA_{254}$ is higher in RW (average values of 2.7 $m^2\ g^{-1}$ in both February and July) than in SW (average values of 0.9 $m^2\ g^{-1}$ in February and 1.0 $m^2\ g^{-1}$ in July) (Table 2 and Fig. 5B and D). Interestingly, between stations 0 and 13 values are markedly lower in July (1.9 $m^2\ g^{-1}$) than in February (2.7 $m^2\ g^{-1}$).

3.3. FDOM

3.3.1 EEMs

EEMs from distinct DOM sources shows interesting differences (Fig. 6), supporting that the different quality of DOM depends on the main source. EEMs in RW (station 0 in February) have 2 main peaks at $\lambda_{ex}/\lambda_{em}$ = 250/400-500 nm and $\lambda_{ex}/\lambda_{em}$ = 320/400-460 nm, that can be related to humic-like fluorophores (A and M according to (Coble, 1996) and α' and β, respectively, according to (Parlanti et al., 2000)). EEMs in SW (station 15-surface in both periods) have 1 main peak at $\lambda_{ex}/\lambda_{em}$ = 270/340 nm analogous to protein-like (tryptophan) fluorophore (T according to (Coble, 1996) and δ according to (Parlanti et al., 2000)) and a small peak at $\lambda_{ex}/\lambda_{em}$ = 250/400-500 nm, due to humic-like fluorophores. EEMs at station 6-surface are clearly different in the two seasons. In February, EEM is similar to that measured in RW, whereas in July a marked peak is observed at $\lambda_{ex}/\lambda_{em}$ = 270/340 nm.

The EEM of the sample collected at station K4, where the phytoplankton bloom occurred, looks different from the others, with very high fluorescence intensity and 3 peaks ($\lambda_{ex}/\lambda_{em}$ = 250/400-460 nm, $\lambda_{ex}/\lambda_{em}$ = 320/380-420 nm and $\lambda_{ex}/\lambda_{em}$ = 270/340 nm), indicating the in-situ production of both humic-like and protein-like substances during the bloom. Interestingly, maximum intensity during the bloom shows peak at $\lambda_{ex}/\lambda_{em}$ = 320/380-420 nm related to marine humic-like fluorophore (M according to (Coble, 1996) and β according to (Parlanti et al., 2000)). Finally, the EEM of the sample collected in the hypoxic waters (station 1-bottom) shows the highest fluorescence intensity and the same 3 peaks observed in the bloom, but with the predominance of humic-like fluorescence at $\lambda_{ex}/\lambda_{em}$ = 250/400-460 nm (fluorophore A according to (Coble, 1996) and α' according to (Parlanti et al., 2000)).

3.3.2 PARAFAC components

PARAFAC applied to the complete dataset (Dataset 1) validated a 3-component model (Table 1) (excitation and emission spectra are given in Fig S2). Component 1 (C1) with Ex_{max}/Em_{max} = 305/416 was identified as microbial humic-like, component 2 (C2) with Ex_{max}/Em_{max} = 275,345/479 as terrestrial humic-like and component 3 (C3) with Ex_{max}/Em_{max} = 275/344 as protein-like (tryptophan).

In February, fluorescence intensity in RW is 0.099 R.U. for C1 and 0.053 R.U. for C2 component, while in July it is 40-50% lower (0.051 R.U. for C1 and 0.032 R.U. for C2 component) (Table 2). C3 component (protein-like) showed the lowest fluorescence in RW in February (0.020 R.U.), whereas it showed 75% increase in July (0.036 R.U.). In comparison to RW, SW shows notably lower fluorescence of all three PARAFAC components in both seasons, with fluorescence values for C1, C2 and C3 component of 0.020, 0.010 and 0.021 R.U. in February and 0.017, 0.009 and 0.016 R.U. in July, respectively. As expected, C2 (terrestrial humic-like) showed the lowest fluorescence in SW.

C1 and C2 have identical distributions with high fluorescence in FWL, decreasing seaward (Fig. 7). In the FWL, humic-like fluorescence (C1 and C2) is significantly lower in July than in February, suggesting their net removal by photobleaching. In contrast, protein-like fluorescence (C3) in FWL, is lower in February than in July, when a marked increase in this component is observed at stations 4-7, suggesting net production of protein-like FDOM in the mixing area. All the 3 components showed a marked increase, in July, at station 1 in the bottom sample, where hypoxia is observed (Fig. 3C), in agreement with DOC and CDOM distribution (Fig. 4C and D).

PARAFAC was applied to different data set in order to investigate if the number and importance of components changed depending on the season or layer. A 6-component model

was validated when the EEMs from July are taken into consideration separately (Dataset 3, Table 1), with 3 new components identified as marine humic-like, terrestrial fulvic-like and PAH-like. Distribution of these components along the estuarine transect is given in Fig. S3. When these samples are further separated by layer, only 3-component model is validated for FWL (Dataset 6), with highest contribution of protein-like fluorescence. However, a 6-component model is still validated for the SWL (Dataset 7), suggesting more complexed DOM pool below the halocline. In contrast, when only the samples collected in winter are taken into consideration (Dataset 2), PARAFAC validates the same 3-component model as with the complete dataset (Dataset 1).

3.4. DOM behavior during estuarine mixing

Distribution of DOC, spectral indices and fluorescence components in salinity gradient is presented in Fig. 8. The linear mixing (conservative behavior) is calculated by linear regression between the two end-members (RW and SW, refer to Table 2 for the values). DOC, a_{254} and protein-like component (C3) show a non-conservative behavior with a clear production of DOC, CDOM and protein-like FDOM at intermediate salinity, in both seasons. The deviation is much more evident in July than in January. Microbial (C1) and terrestrial (C2) humic-like components have the same distribution. For that reason, here is only presented microbial humic-like component (C1). C1 component shows the best fitting with conservative mixing in both seasons, even if in July, values are higher than expected from linear mixing regression.

3.5. Spectral slope curve

SSC is suggested by (Loiselle et al., 2009) as an alternative approach to study absorption characteristics of CDOM instead of using single (or multiple) spectral slopes values. *SSC* could be considered as a fingerprint of the samples, from which different characteristics of the CDOM could be extracted (Loiselle et al., 2009; Massicotte et al., 2017). In the review paper of (Massicotte et al., 2017), the presented average *SSC* (hereafter denoted as *mSSC*) for different water systems spanning aquatic continuum were compared to our *SSC*. In Fig. 9A our typical average *SSCs* were presented for FW and SW. Due to very low absorbance at wavelength higher than 450 nm, the spectral slope is under high influence of the spectral noise and thus these values (potential peaks) should be taken with caution, especially in SW. Relatively good comparison was obtained in terms of the general shape of curves if compared to *mSSC* and SSC from (Loiselle et al., 2009), with slightly higher spectral slope values (S_λ) and ~10 nm shift of peaks towards lower wavelengths. For both curves S_λ is increasing rapidly at low wavelength range, consistent with *mSSC.* As expected, S_λ values

are higher in SW than in FW. Maximal S_λ in FW (0.020 nm^{-1}) is obtained at 300 nm, whereas in SW it is at 290 nm (0.034 nm^{-1}).

The highest differences in *SSC*s of 3 distinctive samples were obtained at wavelengths higher than 300 nm (Fig. 9B), indicating the peaks which reflect occurrence of specific processes. *SSC* of SW sample from hypoxic region showed strong decrease in S_λ if compared to clean SW mainly because of much higher absorbance which progressively increases towards lower spectral range. Especially representative are *SSC*s obtained in the Visovac Lake (station K4) during the bloom and at intermediate salinity (S = 16) during summer production. If compared to winter FW curve (Fig. 9A), *SSC* with pronounced bloom (station K4) showed increase of the peak at 285 nm and appearance of pronounced peak at 370 nm, consistent with the strong increase of fluorescence peak at $\lambda_{ex}/\lambda_{em}$ = 320/380-420 nm (Fig 6). Additional peak was obtained for sample 6-surface at intermediate salinity (S = 16) in July, corresponding to the protein-like peak at $\lambda_{ex}/\lambda_{em}$ = 270/340 nm in EEM (Fig 6). These two atypical peaks are not visible at *mSSC* and could be considered as a site and a process specific. We suggest *SSC* as a fingerprint of the typical samples, since, as presented, there is a clear benefit of *SSC* for identification of potential compounds and related process which could not be observed by using a common discrete spectral slope approach.

4. Discussion

4.1. DOM in the river end-member

The Krka river is one of the major karstic rivers flowing to the middle Adriatic coast, along with the rivers Zrmanja and Cetina. The karst phenomenon of the Croatian Adriatic coast forms systems with self-purifying ability that, added to the very small human impact, makes the Krka River estuary a unique system, very rare in the world and comparable to the world's most pristine riverine systems (Legovic et al., 1994). The riverine waters entering the estuary are characterized by extremely low concentrations of nutrients and terrigenous material (Legovic et al., 1994). Our results clearly show that they are also characterized by very low DOC concentrations. In contrast to most of the rivers all over the world, it therefore has a ″dilution effect″ on marine DOM in the estuary. DOC in the Krka River (30-35 μM) is at least 3-times lower than in the other Mediterranean rivers, especially comparing to the major Mediterranean rivers (Tevere, Po, Ebro and Rhone) with DOC values up to 220 μM (Santinelli, 2015). Extreme case is the Arno River with more than 10-times higher DOC concentrations (320-365 μM) (Retelletti Brogi et al., 2015) than the Krka River. The values reported in our study are lower than those measured by (Strmečki et al., 2018) in the upper reach of the Krka River (Brljan Lake) in March, May, June, September and November of 2011 and in January 2012 (45-127 μM). Despite the wide range of DOC concentrations, 80% of reported

values was lower than 60 µM during their study, whereas values >100 µM were measured only in March and May 2011. The values reported in our study are similar to those measured at the head of the Krka River estuary in February 2012 (35 µM) (Cindric et al., 2015). The difference between DOC concentrations measured in the Lake Brljan and at the head of the estuary can be explained by the cascade of tufa barriers present after the Brljan Lake and to the significant self-purification process that takes place through several small lakes formed along the Krka River flow (Cukrov et al., 2008).

Riverine DOM is characterized by low average $S_{275\text{-}295}$ (16.6 μm^{-1}) and high average $SUVA_{254}$ (2.6 $m^2\ g^{-1}$). $S_{275\text{-}295}$ is used as a proxy of terrestrial DOM and is indirectly correlated to average molecular weight (MW) and aromatic content, while $SUVA_{254}$ indicates the abundance of CDOM in the total DOM pool (Helms et al., 2008; Stedmon and Nelson, 2015). The $S_{275\text{-}295}$ observed at the Krka River estuary are common for terrestrially derived CDOM in real systems (13.5-16.9 μm^{-1}) (Fichot and Benner, 2012), and indicate that DOM in the Krka River is characterized by high average MW and high aromaticity degree. High chromophoric content is highlighted by $SUVA_{254}$ only 10-30% lower than the values found in the pristine Epulu River (Congo) (3-3.6 $m^2\ g^{-1}$), that is characterized by the highest DOC and lignin phenol concentrations of any rainforest (Spencer et al., 2010). DOM pool in the Krka River, also shows a high fluorescence intensity, specifically of PARAFAC components identified as microbial and terrestrial humic-like (C1 and C2).

Seasonality in the river mainly affects DOM quality (FDOM) whereas DOC concentration is very similar in winter and summer. The change in DOM pool is supported by 48.4% and 39.6% reduction in humic-like components (C1 and C2, respectively) and 42.9% increase in protein-like component (C3) in July with respect to February. Due to absence of anthropogenic sources through the whole year (Cukrov et al., 2008) and the low biological activity during the winter (Strmečki et al., 2018), RW contains ″authentic″ terrestrial DOM, whereas production during the spring and summer increases the contribution of autochthonous DOM (Strmečki et al., 2018). Our data support that in-situ production mainly releases protein-like substances, as already observed by (Osburn et al., 2012), making their contribution to the total fluorescence increasing from 11.4% in February to 30.1% in July. The high solar irradiance in summer can further contribute to the change in DOM pool not only stimulating biological production, but also leading to the photodegradation of humic-like substances, that are more susceptible to photodegradation than protein-like substances, due to higher MW and the aromaticity degree (Lee et al., 2018).

4.1.1 DOM in the Visovac Lake

The Visovac Lake (station K4) is located upstream the estuary. It is characterized by intense production and freshwater phytoplankton blooms in spring and summer (Petricioli et al., 1996; Svensen et al., 2007), therefore having a clear effect on chemical and biological properties of RW entering into the estuary. The samples, collected in this lake during the phytoplankton bloom occurring few days before our sampling campaign, allowed us to study DOM properties during the bloom. Visovac Lake is characterized by higher values of chl-*a,* dissolved oxygen and DOC as well as lower chromophoric content (lower $SUVA_{254}$) than surrounding water (stations K1-3 and K5-6) (Fig. 1). Interestingly the Visovac Lake is also characterized by a marked increase in all the components suggesting that in-situ production also releases humic-like components, in agreement with (Bittar et al., 2015) who found that unaltered metabolic product of *M. aeruginosa* shows a fluorescent peaks in region as that of terrestrial humic-like fluorophores. Due to the freshwater phytoplankton blooms, the Visovac Lake influence the quality of DOM in the RW. As a consequence, station 0, which is usually considered as riverine end-member shows different DOM quality depending on the season. While in winter it can be considered as a riverine end-member, since it mainly contains terrestrial DOM, in summer it is strongly affected by in-situ production. For this reason, in summer we used station K1 as representative for riverine DOM instead of station 0. DOC concentration further supports the impact of bloom in the lake on DOM dynamics. At the head of the estuary (station 0) DOC is 17 µM higher in July (55 µM) than in February (38 µM), supporting in-situ net production. These results are in agreement with (Cindric et al., 2015) who reported seasonal difference in DOC concentrations at the station 0 as a consequence of the higher biological activity in summer.

4.2. DOM in the seawater end-member

DOC concentrations in SW (60-63 µM) are higher than in RW but comparable to DOC concentrations measured in the upper layer (0–100 m) of Mediterranean Sea (Med Sea) (58±7 µM for Western Med and 59±6 for Eastern Med µM) (Santinelli, 2015). CDOM absorption, as well as $SUVA_{254}$ and $S_{275\text{-}295}$ values in SW (Table 1) correspond to the upper range of values reported by (Galletti et al., 2019) for open waters of the Med Sea. Absorption values are slightly higher, while $S_{275\text{-}295}$ values are in the lower range of values reported by (Catala et al., 2018). In SW, DOM pool is characterized by average MW and chromophoric content lower than in RW as suggested by 2-times higher average $S_{275\text{-}295}$ (29.3-30.5 μm^{-1}) and 3-times lower $SUVA_{254}$ (0.9-1.0 $m^2\ g^{-1}$). Open waters of the Med Sea generally show lower CDOM absorption than coastal areas impacted by river input and the other marginal seas (Table 4 in (Galletti et al., 2019)). CDOM data observed in this study suggest that coastal area has low terrestrial influence comparing to data reported for marginal seas with a clear

riverine signature (e.g. Baltic, North, Black Sea) (Table 4. in (Galletti et al., 2019)). In July, photochemical processes affect DOM pool resulting in slight decrease in fluorescence of all PARAFAC components comparing to February (6-24%), although the contribution of single component to the total fluorescence remained relatively the same.

4.3. DOM in the surface fresh/brackish water layer

DOM shows non-conservative mixing between the two end-members (RW and SW) in both sampling. In the mixing area (S = 15-18) net production is suggested by the marked increase in DOC, a_{254} and protein-like fluorescence with respect to linear mixing (Fig. 8). Interestingly, the correlation between DOC and a_{254} is direct in July, suggesting that the dynamics of DOC and CDOM is coupled with the net production of both, whereas in February an inverse correlation was observed with increasing a_{254} at low DOC concentration (Fig. 10). This correlation indicates that despite the in-situ production, the main effect on DOM dynamics is the mixing between RW (low DOC and high a_{254}) and SW (high DOC and low a_{254}). These seasonal variations are the result of changes in river discharge and high temperature in summer. The Krka estuary is characterized by high riverine input in winter, which brings terrestrial DOM into the estuary. Conversely, in summer, low river discharge results in extended water residence time, that in addition to the high temperature, is favoring biological productivity in Visovac Lake as well as in the estuary (Legovic et al., 1994), leading to in-situ production of DOM.

In July, the highest DOC concentration (up to 147 µM) is in the FWL between stations 5 and 7 (Fig. 4C). The water column is well stratified due to the occurrence of a marked halocline at about 1.5 m (Fig. 2C). DOC accumulation in the FWL can be explained by a decoupling between production and removal processes. As above reported, the increase in production can be explained by the freshwater phytoplankton bloom, since a direct release of DOM has been observed by active growing phytoplankton (Carlson and Hansell, 2015) as well as by the decomposition of dead freshwater phytoplankton (Vilicic et al., 1989). The increase in salinity leads to the mortality of freshwater phytoplankton that can represent a relevant source of DOC. (Vilicic et al., 1989) showed that the ratio between chl-*a* and phaeophytin (chlorophyll degradation product) rapidly decreases at the halocline, suggesting a high proportion of dead phytoplankton. Their microscopic observations confirmed the presence of dead cells along with active phytoplankton in the freshwater-seawater interface. DOC accumulation is always observed above the halocline in stratified systems and often is not in correspondence with chl-*a* concentrations (Santinelli et al., 2013). We cannot exclude that further increase in DOC concentrations in upper layer during high stratification may come from atmospheric deposition (Ternon et al., 2010). On the other side, the accumulation can

be explained by the inability of bacteria to use the DOC, leading to its accumulation in the FWL.

Possible reasons for lack of bacterial removal are: (1) nutrient limitation due to the enhanced stratification in July, that limits the nutrient supply to the surface waters, (2) stress caused by the change in salinity, (3) high irradiation inhibiting bacterial growth, (4) photochemical transformation of DOM from labile to recalcitrant, that is not available to bacteria on the short temporal scale (Jiao et al., 2010; Santinelli et al., 2013), (5) high grazing and viral lysis of bacteria. Probably all the above processes together can explain the observed pattern. While in other estuarine systems, such as Arno river (Gonnelli et al., 2013), enrichment in nutrients and organic matter can stimulate the growth of the bacteria enabling them to resist the salinity shock, in the Krka estuary nutrient limitation in FWL, along with high solar irradiation during the summer, could result in extremely low bacterial activity above the halocline. (Santinelli et al., 2013). Additionally, the possibly higher optical transparency of surface waters would increase the importance of photochemical reactions transforming the structure of DOM and increasing the refractory fraction (Jiao et al., 2010; Santinelli et al., 2013).The high fluorescence of protein-like component (C3) in the FWL supports the hypothesis that there is limitation of bacterial growth, since the protein like components are known to be the most labile fraction of DOM that are first removed by bacterial degradation (Fellman et al., 2011). Additional data, such as nutrient concentrations, bacterial, phytoplankton, zooplankton and virus abundance as well as bacterial production are mandatory in order to explain the non-conservative behavior in the estuary and the observed in-situ production.

4.4. DOM in the bottom seawater layer

Chl-*a* profile suggests that the highest phytoplankton activity is near the bottom in the seawater (Fig. 3D). The same chl-*a* distribution was observed in previous cruises (July 2017 and July 2018) (Fig. S5). Entering the estuary, the increased salinity causes mortality of freshwater phytoplankton and half of the cells sink to the bottom before Prokljan Lake, where they serve as a nutrient source for marine phytoplankton below the halocline (Legovic et al., 1991; Petricioli et al., 1996). The availability of both nutrients and light can stimulate marine phytoplankton explaining the high chl-*a* values in the deeper SWL. We would therefore expect DOM in-situ production in this layer. In the landward direction, DOC increases to values >80 µM at stations 1-4 (Fig. 4C and Table 3), suggesting in-situ production. The increase in DOC is, however, less marked than that observed in the FWL, despite the higher values of chl-*a*. This difference can be explained by the different source of DOM, that is marine blooming phytoplankton in SWL and dead freshwater phytoplankton in RWL. In

addition, in the SWL bacteria removal of DOM is expected to be more active due to the availability of nutrients and the lower light intensity. This hypothesis is supported by the values of the apparent oxygen utilization (AOU), that gives an indirect information about oxygen consumption and can be transformed in C equivalent, that is the amount of DOC removed to explain the apparent oxygen consumption. AOU is high at stations 5-10, where, despite the high chl-*a*, no marked increase in DOC was observed (Table 3). However, if the AOU C_{eq} are added to the DOC values measured at these stations, we obtain values comparable to those measured at stations 2-4 supporting that microbial respiration can explain the discrepancy between the high values of chl-*a* and the lower than expected increase in DOC.

4.5. DOM in the hypoxic waters

In our study, in the inner part of the estuary, oxygen saturation shows values <75% in February, whereas decreases below 38% in July at station 1 (Fig. 3A and C). This site is characterized by a specific cuvette shape, in which the residence time of the seawater is probably increased comparing to adjacent seawater (Cindric et al., 2015). As a result of longer seawater residence time in summer, sinking of decaying FW phytoplankton along with the organic detritus from the upper layer and its accumulation at the bottom, enhances the effect of bacterial mineralization causing oxygen depletion. In case of particularly high production in the Visovac Lake and within the estuary, hypoxia can be observed in late summer and autumn in the shallow part of the estuary (stations 1-5) (Legovic et al., 1991; Petricioli et al., 1996). In winter, the inflow of the freshwater promotes the seawater renewal and ventilation. Taking into consideration the samples with oxygen saturation <75%, a positive correlation between oxygen saturation, DOC, a_{254}, $SUVA_{254}$ and all three PARAFAC components is observed, with R^2 values of 0.99 (Fig. S6). The lowest oxygen saturation is followed by 46% higher DOC and 75-77% higher CDOM and FDOM compared to the highest oxygen saturation among this samples. Even if the data are not enough for a meaningful investigation of the processes leading to DOM accumulation, the very good correlation suggests that the oxygen removal is coupled with the production of DOM with high percentage of CDOM and FDOM in hypoxic waters. This observation is in agreement with (Margolin et al., 2016), who found strong correlations between optical properties and mineralization in anoxic waters in Black Sea. They also observed higher increase in CDOM and humic-like FDOM than in DOC, due to the release of CDOM during organic matter mineralization or by the microbial transformation of non-chromophoric DOM into CDOM.

5. Conclusion

Our data support that the Krka River estuary is affected by different sources of DOM with distinct optical properties. DOM pool in the river, despite the very low concentration, mainly contains terrestrial molecules, as suggested by the high chromophoric content, high $SUVA_{254}$ and low $S_{275-295}$ values, as well by the predominance of humic-like substances. DOM in the seawater features the concentration and optical properties of the "typical" DOM from open sea waters. In-situ production of DOM is clearly observed in the estuary, leading to a non-conservative behavior, in particular in summer. The increase in the predominance of protein-like substances supports that DOM is mainly released by biological processes. The high concentrations observed in the freshwater layer in summer are probably due to the low efficiency of heterotrophic prokaryotes in the removal of the produced DOM, determining its accumulation, however biological data are mandatory to support this hypothesis.

Our study shows that the Krka River estuary is a very interesting system, where the main processes affecting DOM dynamics can be studied in detail. It can therefore be a model site for studies on the behavior and fate of different DOM pools. For the future it is crucial to combine study on DOM with biological information, such as heterotrophic prokaryotes abundance and production, primary production as well as phytoplankton and zooplankton abundance, in order to gain insights into the main processes that can explain DOM accumulation and fate in the estuary and to investigate their impact on the global carbon cycle.

Acknowledgment: This research was realized within the scope of project "New methodological approach to biogeochemical studies of trace metal speciation in coastal aquatic ecosystems" (MEBTRACE), financially supported by the Croatian Science Foundation under the project number IP-2014-09-7530.

Literature:

Bittar, T.B., Vieira, A.A., Stubbins, A. and Mopper, K., 2015. Competition between photochemical and biological degradation of dissolved organic matter from the cyanobacteria Microcystis aeruginosa. Limnology and Oceanography, 60(4): 1172-1194.

Buzancic, M., Gladan, Z.N., Marasovic, I., Kuspilic, G. and Grbec, B., 2016. Eutrophication influence on phytoplankton community composition in three bays on the eastern Adriatic coast. Oceanologia, 58(4): 302-316.

Carlson, C.A. and Hansell, D.A., 2015. DOM sources, sinks, reactivity, and budgets, Biogeochemistry of marine dissolved organic matter. Elsevier, pp. 65-126.

Catala, T.S. et al., 2018. Dissolved Organic Matter (DOM) in the open Mediterranean Sea. I. Basin-wide distribution and drivers of chromophoric DOM. Progress in Oceanography, 165: 35-51.

Cetinic, I., Vilicic, D., Buric, Z. and Olujic, G., 2006. Phytoplankton seasonality in a highly stratified karstic estuary (Krka, Adriatic Sea). Hydrobiologia, 555: 31-40.

Cindric, A.M., Garnier, C., Oursel, B., Pizeta, I. and Omanovic, D., 2015. Evidencing the natural and anthropogenic processes controlling trace metals dynamic in a highly stratified estuary: The Krka River estuary (Adriatic, Croatia). Marine Pollution Bulletin, 94(1-2): 199-216.

Coble, P.G., 1996. Characterization of marine and terrestrial DOM in seawater using excitation emission matrix spectroscopy. Marine Chemistry, 51(4): 325-346.

Cukrov, N., Cmuk, P., Mlakar, M. and Omanovic, D., 2008. Spatial distribution of trace metals in the Krka River, Croatia: An example of the self-purification. Chemosphere, 72(10): 1559-1566.

Dainard, P.G., Guéguen, C., McDonald, N. and Williams, W.J., 2015. Photobleaching of fluorescent dissolved organic matter in Beaufort Sea and North Atlantic Subtropical Gyre. Marine Chemistry, 177: 630-637.

Dixon, J.L., Osburn, C.L., Paerl, H.W. and Peierls, B.L., 2014. Seasonal changes in estuarine dissolved organic matter due to variable flushing time and wind-driven mixing events. Estuarine, Coastal and Shelf Science, 151: 210-220.

Fellman, J.B., Petrone, K.C. and Grierson, P.F., 2011. Source, biogeochemical cycling, and fluorescence characteristics of dissolved organic matter in an agro-urban estuary. Limnology and Oceanography, 56(1): 243-256.

Fichot, C.G. and Benner, R., 2012. The spectral slope coefficient of chromophoric dissolved organic matter (S275–295) as a tracer of terrigenous dissolved organic carbon in river-influenced ocean margins. Limnology and Oceanography, 57(5): 1453-1466.

Galletti, Y., Gonnelli, M., Brogi, S.R., Vestri, S. and Santinelli, C., 2019. DOM dynamics in open waters of the Mediterranean Sea: New insights from optical properties. Deep-Sea Research Part I-Oceanographic Research Papers, 144: 95-114.

Gonnelli, M., Vestri, S. and Santinelli, C., 2013. Chromophoric dissolved organic matter and microbial enzymatic activity. A biophysical approach to understand the marine carbon cycle. Biophysical Chemistry, 182: 79-85.

Grzetic, Z., Precali, R., Degobbis, D. and Skrivanic, A., 1991. Nutrient Enrichment and Phytoplankton Response in an Adriatic Karstic Estuary. Marine Chemistry, 32(2-4): 313-331.

Hansell, D.A., Carlson, C.A., Repeta, D.J. and Schlitzer, R., 2009. Dissolved organic matter in the ocean: A controversy stimulates new insights. Oceanography, 22(4): 202-211.

Helms, J.R. et al., 2008. Absorption spectral slopes and slope ratios as indicators of molecular weight, source, and photobleaching of chromophoric dissolved organic matter. Limnology and Oceanography, 53(3): 955-969.

Jiao, N. et al., 2010. Microbial production of recalcitrant dissolved organic matter: long-term carbon storage in the global ocean. Nature Reviews Microbiology, 8(8): 593.

Knežević, L., Cukrov, N. and Bura-Nakić, E., 2019. Ion-exchange chromatography as a tool for investigating vanadium speciation in sediments: preliminary studies. Journal of Soils and Sediments: 1-8.

Lee, M.H., Osburn, C.L., Shin, K.H. and Hur, J., 2018. New insight into the applicability of spectroscopic indices for dissolved organic matter (DOM) source discrimination in aquatic systems affected by biogeochemical processes. Water Research, 147: 164-176.

Legovic, T., 1991. Exchange of Water in a Stratified Estuary with an Application to Krka (Adriatic Sea). Marine Chemistry, 32(2-4): 121-135.

Legovic, T., Petricioli, D. and Zutic, V., 1991. Hypoxia in a Pristine Stratified Estuary (Krka, Adriatic Sea). Marine Chemistry, 32(2-4): 347-359.
Legovic, T. et al., 1994. Eutrophication in the Krka Estuary. Marine Chemistry, 46(1-2): 203-215.
Loiselle, S.A. et al., 2009. Optical characterization of chromophoric dissolved organic matter using wavelength distribution of absorption spectral slopes. Limnology and Oceanography, 54(2): 590-597.
Margolin, A.R., Gerringa, L.J.A., Hansell, D.A. and Rijkenberg, M.J.A., 2016. Net removal of dissolved organic carbon in the anoxic waters of the Black Sea. Marine Chemistry, 183: 13-24.
Massicotte, P., Asmala, E., Stedmon, C. and Markager, S., 2017. Global distribution of dissolved organic matter along the aquatic continuum: Across rivers, lakes and oceans. Science of the Total Environment, 609: 180-191.
Murphy, K.R., Stedmon, C.A., Graeber, D. and Bro, R., 2013. Fluorescence spectroscopy and multi-way techniques. PARAFAC. Analytical Methods, 5(23): 6557-6566.
Murphy, K.R., Stedmon, C.A., Wenig, P. and Bro, R., 2014. OpenFluor- an online spectral library of auto-fluorescence by organic compounds in the environment. Analytical Methods, 6(3): 658-661.
Omanović, D., Santinelli, C., Marcinek, S. and Gonnelli, M., 2019. ASFit - An all-inclusive tool for analysis of UV–Vis spectra of colored dissolved organic matter (CDOM). Computers & Geosciences, accepted.
Osburn, C.L., Handsel, L.T., Mikan, M.P., Paerl, H.W. and Montgomery, M.T., 2012. Fluorescence tracking of dissolved and particulate organic matter quality in a river-dominated estuary. Environmental science & technology, 46(16): 8628-8636.
Pađan, J. et al., 2019a. Determination of sub-picomolar levels of platinum in the pristine Krka River estuary (Croatia) using improved voltammetric methodology. Environmental Chemistry.
Pađan, J. et al., 2019b. Improved voltammetric methodology for chromium redox speciation in estuarine waters. Analytica Chimica Acta, 1089: 40-47.
Parlanti, E., Worz, K., Geoffroy, L. and Lamotte, M., 2000. Dissolved organic matter fluorescence spectroscopy as a tool to estimate biological activity in a coastal zone submitted to anthropogenic inputs. Organic Geochemistry, 31(12): 1765-1781.
Petricioli, D., BakranPetricioli, T., Vilicic, D. and PozarDomac, A., 1996. Freshwater phytoplankton bloom in Visovac lake - A possible cause of benthic mortality in Krka estuary (Adriatic sea, Croatia). Marine Ecology-Pubblicazioni Della Stazione Zoologica Di Napoli I, 17(1-3): 373-382.
Repeta, D.J., 2015. Chemical characterization and cycling of dissolved organic matter, Biogeochemistry of marine dissolved organic matter. Elsevier, pp. 21-63.
Retelletti Brogi, S., Gonnelli, M., Vestri, S. and Santinelli, C., 2015. Biophysical processes affecting DOM dynamics at the Arno river mouth (Tyrrhenian Sea). Biophysical Chemistry, 197: 1-9.
Santinelli, C., 2015. Chapter 13 - DOC in the Mediterranean Sea. In: D.A. Hansell and C.A. Carlson (Editors), Biogeochemistry of Marine Dissolved Organic Matter (Second Edition). Academic Press, Boston, pp. 579-608.

Santinelli, C., Follett, C., Brogi, S.R., Xu, L. and Repeta, D., 2015. Carbon isotope measurements reveal unexpected cycling of dissolved organic matter in the deep Mediterranean Sea. Marine Chemistry, 177: 267-277.

Santinelli, C., Hansell, D.A. and d'Alcalà, M.R., 2013. Influence of stratification on marine dissolved organic carbon (DOC) dynamics: The Mediterranean Sea case. Progress in oceanography, 119: 68-77.

Santinelli, C., Nannicini, L. and Seritti, A., 2010. DOC dynamics in the meso and bathypelagic layers of the Mediterranean Sea. Deep Sea Research Part II: Topical Studies in Oceanography, 57(16): 1446-1459.

Santos, L. et al., 2016. Insights on the Optical Properties of Estuarine DOM - Hydrological and Biological Influences. Plos One, 11(5).

Spencer, R.G.M. et al., 2010. Temporal controls on dissolved organic matter and lignin biogeochemistry in a pristine tropical river, Democratic Republic of Congo. Journal of Geophysical Research: Biogeosciences, 115(G3).

Stedmon, C.A. and Nelson, N.B., 2015. The optical properties of DOM in the ocean, Biogeochemistry of Marine Dissolved Organic Matter. Elsevier, pp. 481-508.

Strmečki, S. et al., 2018. Voltammetric study of organic matter components in the upper reach of the Krka River, Croatia. Croatica Chemica Acta, 91(4): 1-8.

Supraha, L. et al., 2014. Cryptophyte bloom in a Mediterranean estuary: High abundance of Plagioselmis cf. prolonga in the Krka River estuary (eastern Adriatic Sea). Scientia Marina, 78(3): 329-338.

Svensen, C., Vilicic, D., Wassmann, P., Arashkevich, E. and Ratkova, T., 2007. Plankton distribution and vertical flux of biogenic matter during high summer stratification in the Krka estuary (Eastern Adriatic). Estuarine Coastal and Shelf Science, 71(3-4): 381-390.

Ternon, E. et al., 2010. The impact of Saharan dust on the particulate export in the water column of the North Western Mediterranean Sea. Biogeosciences, 7(3): 809-826.

Vilicic, D., Legovic, T. and Zutic, V., 1989. Vertical-Distribution of Phytoplankton in a Stratified Estuary. Aquatic Sciences, 51(1): 31-46.

Yamashita, Y., Panton, A., Mahaffey, C. and Jaffé, R., 2011. Assessing the spatial and temporal variability of dissolved organic matter in Liverpool Bay using excitation–emission matrix fluorescence and parallel factor analysis. Ocean Dynamics, 61(5): 569-579.

Zutic, V. and Legovic, T., 1987. A Film of Organic-Matter at the Fresh-Water Sea-Water Interface of an Estuary. Nature, 328(6131): 612-614.